Generalized dissipation dilution in strained mechanical resonators

S. A. Fedorov, N. J. Engelsen, A. H. Ghadimi, M. J. Bereyhi, R. Schilling, D. J. Wilson, and T. J. Kippenberg

Phys. Rev. B **99**, 054107 — Published 28 February 2019

DOI: 10.1103/PhysRevB.99.054107

Generalized dissipation dilution in strained mechanical resonators

S. A. Fedorov,[1] N. J. Engelsen,[1] A. H. Ghadimi,[1] M. J. Bereyhi,[1] R. Schilling,[1] D. J. Wilson,[2] and T. J. Kippenberg[1]

[1] *Institute of Physics (IPHYS), École Polytechnique Fédérale de Lausanne, 1015 Lausanne, Switzerland*
[2] *IBM Research — Zurich, Saümerstrasse 4, 8803 Rüschlikon, Switzerland*

(Dated: February 12, 2019)

Mechanical resonators with high quality factors are widely used in precision experiments, ranging from gravitational wave detection and force sensing to quantum optomechanics. Beams and membranes are well known to exhibit flexural modes with enhanced quality factors when subjected to tensile stress. The mechanism for this enhancement has been a subject of debate, but is typically attributed to elastic energy being "diluted" by a lossless potential. Here we clarify the origin of the lossless potential to be the combination of tension and geometric nonlinearity of strain. We present a general theory of dissipation dilution that is applicable to arbitrary resonator geometries and discuss why this effect is particularly strong for flexural modes of nanomechanical structures with high aspect ratios. Applying the theory to a non-uniform doubly clamped beam, we show analytically how dissipation dilution can be enhanced by modifying the beam shape to implement "soft clamping", thin clamping and geometric strain engineering, and derive the ultimate limit for dissipation dilution.

I. INTRODUCTION

Mechanical resonators with high quality factors are of both fundamental and applied interest. They are employed in gravitational waves detectors [1], cavity optomechanics [2], quantum [3] and classical [4] signal conversion, tests of wavefunction collapse models [5] and numerous sensing applications [6, 7]. In all these endeavors, dissipation can be a limiting factor. As known from the fluctuation-dissipation theorem [8], dissipation introduces noise, which limits force sensitivity, frequency stability and results in decoherence of quantum states. Reduction of mechanical dissipation is practically challenging, however, because intrinsic and surface loss mechanisms are often not well understood or not possible to control. The quality factor, Q, of a mechanical resonator typically does not exceed the inverse of the material loss angle, ϕ, characterizing the delay between stress and strain. Flexural modes of beams and membranes under tension are notable exceptions to this rule: they can have Qs far in excess of $1/\phi$ due to a phenomenon known as *dissipation dilution*.

The origin of dissipation dilution has been a subject of debate. The concept was introduced in the gravitational wave community when, to explain the enhanced Q of test mass suspension wire, Gonzalez *et. al.* [9, 10] reasoned that the lossy elastic energy of the wire was "diluted" by the conservative gravitational potential of the test mass. A decade later, similar behavior was observed in nanometric strings and membranes made of highly-strained materials (most notably, silicon nitride [11–13]); however, the lack of an external potential in this case necessitated a rethinking of the physical model. In later works the quality factors of flexural modes of uniform beams [14] and membranes [15] were calculated from a structural mechanics perspective and shown to be much greater than $1/\phi$—in excellent agreement with experiments [14–17]. These results partially demystified dissipation dilution, but due to their lack of generality, the understanding of this effect remains incomplete. It is still not fully clear what causes dissipation dilution to emerge in a resonator (aside from the mere presence of tensile strain), whether any non-flexural modes experience dilution and to what extent it can be engineered to produce practical high-Q resonators.

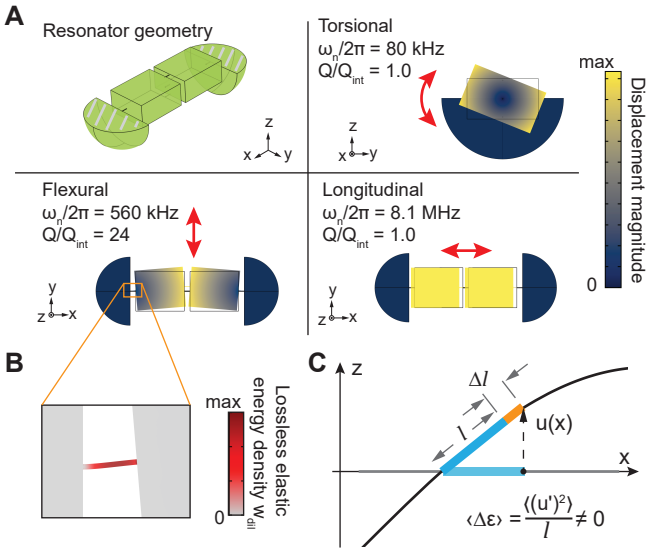

FIG. 1. A) Dissipation dilution factors for vibrational modes of a 3D resonator, doubly clamped to two quarter-sphere pads (hatched gray) and subjected to tension. The total length is 20 μm, the block size is $8.5 \times 7 \times 4$ μm, the bridge diameter is 100 nm and the material pre-strain is 0.4%. B) Distribution of effectively lossless elastic energy in a thin bridge during flexural vibration. C) Schematic illustrating how the cycle-averaged dynamic strain $\langle \Delta\epsilon \rangle$ can be non-zero due to geometric nonlinearity.

Very recently, dissipation dilution has attracted significant interest as it enabled nanomechanical resonators, in the form of patterned membranes and beams, to achieve exceptionally high Q factors [18, 19]. In particular, by

localizing a beam mode away from its supports with a phononic crystal (the "soft clamping" approach introduced by Tsaturyan et al. [18, 20]) and using geometric strain engineering [21] to enhance strain in the beam constriction, Q factors as high as 8×10^8 were demonstrated at room temperature [19]—surpassing even the highest values measured in macroscopic sapphire bars [22]. These advances suggest that a more detailed understanding of dissipation dilution may be beneficial for optimizing existing designs and finding new ones, in addition to answering the open questions mentioned above.

Here we address these questions with a general and consistent theory which does not resort to the concept of an *a priori* lossless potential. We derive the dissipation dilution factors for modes of a mechanical resonator of arbitrary geometry. We identify *geometric nonlinearity* of strain in deformations to be a key component which, together with static strain, enables dissipation dilution. We extend the classic treatment of Q dilution in flexural vibrations of a doubly-clamped beam to the case where the beam has a non-uniform width. Using this theory we show how a non-uniform width can be used to enhance Q with three strategies: mode localization with phononic crystals [18], both alone and in combination with adiabatic tapering [19] and "thin clamping", introduced here. We show that in a number of cases engineering dissipation dilution is related to geometric strain engineering [23, 24]. We also derive the ultimate limit of dissipation dilution set by the material yield strain. Our numerical analysis of beams is based on the one-dimensional Euler-Bernoulli equation and is in excellent agreement with a full 3D treatment. The numerical routines for nanobeam Q factor calculations are implemented in a freely available `Mathematica` package [25].

II. GEOMETRIC ORIGIN OF DISSIPATION DILUTION

Dissipation dilution is commonly illustrated by a harmonic oscillator subjected to an external lossless potential [9], as in the case of optically-trapped mirrors [26, 27] or massive pendula in a gravitational field [9]. If $\omega_{\rm int}$ is the oscillator natural frequency, ϕ is its loss angle [28] and $\omega_{\rm dil}$ is the frequency of motion in the lossless potential, then the oscillator Q factor is increased compared to the intrinsic value $Q_{\rm int}\equiv1/\phi$ by the "dilution factor",

$$D_Q\equiv\frac{Q}{Q_{\rm int}}=\frac{\omega_{\rm int}^2+\omega_{\rm dil}^2}{\omega_{\rm int}^2}. \tag{1}$$

For flexural vibrations of tensioned beams or membranes, the Q enhancement takes place similarly to Eq. 1 with the important distinction that here the potential energy is stored only as elastic energy. Instead of introducing an external potential, the elastic energy is divided into lossy "bending" and lossless "tension" parts [14, 15], related to the curvature and gradient of the mode shape, respectively. It is not evident a priori, however, how to make this separation in a general case and under which conditions the lossless part of energy is non-zero. Here we answer both questions and show that the effectively lossless elastic energy emerges if two conditions are satisfied: a) static strain is non-zero in the resonator and b) the average of strain variation over the oscillation period is non-zero, i.e. the geometric nonlinearity of strain is significant.

We now derive the dissipation dilution factor of a generic vibrational mode. For this we compute the Q factor as the ratio of the elastic energy stored by the mode to the energy dissipated per vibrational period. We assume that static deformation is present in the structure along with a part oscillating at the frequency ω_n. Denoting the total deformation field as $\tilde{U}_i(x,y,z,t)$ $(i=x,\,y,\,z)$, the strain tensor $\tilde{e}_{ij}$ [29] is given by

$$\tilde{e}_{ij}=\frac{1}{2}\left(\frac{\partial\tilde{U}_i}{\partial x_j}+\frac{\partial\tilde{U}_j}{\partial x_i}+\frac{\partial\tilde{U}_l}{\partial x_i}\frac{\partial\tilde{U}_l}{\partial x_j}\right), \tag{2}$$

where summation over repeating indices is implied. The last term in Eq. 2 is nonlinear in the displacement and can be identified as the geometric nonlinearity. We emphasize here that this nonlinearity is not due to a nonlinear stress-strain relation and is not always negligible for infinitesimally small vibrations.

The strain tensor can be split into static e_{ij} and time-dependent $\Delta e_{ij}(t)$ contributions

$$\tilde{e}_{ij}(t)=e_{ij}+\Delta e_{ij}(t). \tag{3}$$

For brevity, when treating the 3D case we present a simplified model where Poisson's ratio, ν, is neglected, so that the stress-strain relation is given by

$$\tilde{\sigma}_{ij}[\omega]=Ee^{-i\phi}\tilde{e}_{ij}[\omega]. \tag{4}$$

A full treatment accounting for Poisson's ratio can be found in the Supplementary Information[30] and it is included below when treating flexural modes of beams.

We find the time-averaged elastic energy density stored by the mode as

$$\langle\Delta w_{\rm el}(t)\rangle=E\frac{\langle\tilde{e}_{ij}(t)\tilde{e}_{ij}(t)\rangle}{2}-E\frac{e_{ij}e_{ij}}{2}= E\left(e_{ij}\langle\Delta e_{ij}(t)\rangle+\frac{\langle\Delta e_{ij}(t)\Delta e_{ij}(t)\rangle}{2}\right), \tag{5}$$

and the dissipated power density $p_{\rm diss}$ as

$$p_{\rm diss}=\langle\tilde{\sigma}_{ij}(t)\,(\tilde{e}_{ij})'_t(t)\rangle=\omega_n\,\phi\,E\langle\Delta e_{ij}(t)\Delta e_{ij}(t)\rangle. \tag{6}$$

The dilution factor of the vibrational mode is given by the ratio of the resonator quality factor to $Q_{\rm int}$ as

$$D_Q=1+\frac{\int 2e_{ij}\langle\Delta e_{ij}(t)\rangle dV}{\int\langle\Delta e_{ij}(t)\Delta e_{ij}(t)\rangle dV}. \tag{7}$$

Eq. 7 reveals the peculiar effect of static strain e_{ij} on dissipation. If the static strain is zero then $D_Q=$

$Q/Q_{\mathrm{int}} = 1$ irrespective of the mode shape (we emphasize that corrections due to the imaginary part of Poissons ratio are here neglected). In contrast, D_Q can be higher (or lower) than unity if $e_{ij} \neq 0$ and $\langle \Delta e_{ij}(t) \rangle \neq 0$, the latter being possible due to geometric nonlinearity in Eq. 2.

Comparing Eq. 7 to Eq. 1, one recognizes

$$\langle W_{\mathrm{dil}}(t) \rangle \equiv E \int e_{ij} \langle \Delta e_{ij}(t) \rangle dV \tag{8}$$

as an effectively lossless potential that generalizes the "tension energy" in treatment of beams and membranes [10, 15]. The lossy part of the energy is given by

$$\langle W_{\mathrm{lossy}}(t) \rangle \equiv \frac{E}{2} \int \langle \Delta e_{ij}(t) \Delta e_{ij}(t) \rangle dV, \tag{9}$$

which generalizes the "bending energy" [10, 15] and corresponds to ω_{int}^2 in Eq. 1. Unlike the toy model, however, W_{lossy} in general depends on the static strain, which implies that the intuitive picture that tension increases stored energy without affecting dissipation is not correct in general.

To give an example, we apply Eq. 7 (more precisely, its counterpart accounting for ν given by Eq. SI13 in Supplementary Information[30]) to a clamped 3D resonator made of pre-strained material shown in Fig. 1A and calculate dilution factors for a few representative modes from different families. It can be seen that among these modes only the flexural ones experiences dissipation dilution, whereas the torsional and longitudinal modes do not. A visualization of lossless energy density $\langle w_{\mathrm{dil}}(t) \rangle$ in Fig. 1B shows that the lossless potential is concentrated in thin bridges between the blocks. This is explained by a) static strain concentration in constrictions and b) relatively large geometric nonlinearity of strain in flexural deformations, as opposed to torsional or longitudinal deformations.

Strong dissipation dilution of flexural modes in high-aspect-ratio beams and membranes [12, 14] is thus due to the combination of tension and a large geometrically nonlinear contribution to the dynamic strain. The latter can be illustrated by considering flexural deformation of an idealized infinitely thin beam shown in Fig. 1C. If the beam is oriented along the x-axis and vibrates along the z-direction with magnitude u, only the diagonal component $\tilde{e}_{xx} \equiv \tilde{\epsilon}$ is relevant and the dynamic variation of strain is quadratic (i.e. fully nonlinear) in the displacement magnitude:

$$\Delta\epsilon(x,t) = (\tilde{u}_x'(x,t))^2/2. \tag{10}$$

Recognizing the role of geometric nonlinearity provides a warning: it is not correct to assume that the mere presence of tensile strain in a mechanical resonator increases its Q—for example, torsional modes of the same structures that have high-Q flexural modes usually do not experience any appreciable dissipation dilution (see Fig. 1A).

Although it does not seem straightforward to come up with a general recipe how to optimally exploit dissipation dilution in an arbitrary structure, in part because the static strain distribution and vibrational mode shape are both affected by resonator geometry, two trends can be nevertheless identified. First, since the nonlinear part of strain tensor is only non-negligible when the linear part is small, dissipation dilution does not typically take place for modes in which the directions of deformation and dynamic strain coincide. To give an example, for a purely dilatational wave propagating in x-direction Eq. 2 yields

$$\tilde{e}_{xx} = \frac{\partial \tilde{U}_x}{\partial x} + \frac{1}{2}\left(\frac{\partial \tilde{U}_x}{\partial x}\right)^2. \tag{11}$$

Here the geometrically nonlinear part is always negligible, unless the static elongation e_{xx} is greater than one, which greatly exceeds the yield strains for most conventional materials. Secondly, a mechanical resonator of strongly non-uniform shape has a strongly inhomogeneous strain distribution with peak values greatly exceeding the average. This limits the acceptable average strain as the peak needs to stay below the material yield value. Therefore unless the vibrational mode is confined inside a region of locally high strain, an overly strong inhomogeneity of the resonator shape is always disadvantageous. This is even more true for the case where the resonator is patterned from a material with fixed pre-strain, as here the average relaxed strain is reduced more for highly non-uniform shapes.

III. DISSIPATION DILUTION OF BEAM RESONATORS

For the rest of the paper we consider in detail the flexural modes of beams, as extreme dissipation dilution is achievable in this case and at the same time a number of analytical results are possible to obtain in addition to those reported in earlier works [10, 16]. Applying Eq. 7 we arrive at a dilution factor given by

$$D_Q = 1 + \frac{\int 2\epsilon \langle \Delta\epsilon(t) \rangle dV}{\int \langle \Delta\epsilon(t)^2 \rangle dV}, \tag{12}$$

where ϵ is the static strain along the beam, terms proportional to $\epsilon\langle\Delta\epsilon(t)\rangle$ and $\langle\Delta\epsilon(t)^2\rangle$ correspond to the lossless "tension" and lossy "bending" energy, respectively [10, 15]—both are of elastic origin. Note that while Eq. 7 neglects Poisson's ratio, Eq. 12 does not, and is formally exact in the 1D case.

So far we have not made any assumptions about the beam cross-section, but in the following we focus on geometries directly accessible by nanofabrication. Specifically, we assume that the beams are made of a suspended film with thickness h and pre-strain $e_{xx} = e_{yy} = \epsilon_{\mathrm{film}}$ (which redistributes upon suspension). The beam width

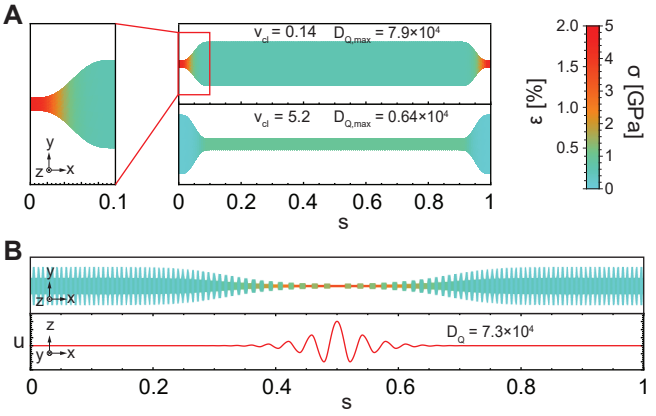

FIG. 2. Geometry, strain distribution and D_Q in micropatterned beams, illustrating the concepts of soft-clamping, thin clamping and strain-engineering. Dilution factors (D_Q) are calculated assuming beam length $l = 3$ mm and thickness $h = 20$ nm. A) Beams with thin (above) and thick (below) clamps, resulting in enhanced and reduced dissipation dilution, respectively. $D_{Q,\max}$ is maximum over modes. B) Strain (top) and localized mode displacement field (bottom) in a tapered phononic crystal beam.

$w(x)$ is in general non-uniform and its variation can be used to improve vibrational quality factors.

For modes of a uniform rectangular beam evaluation of Eq. 12 yields the well-known result [10, 16]

$$D_{Q,n} = \frac{1}{2\lambda + \pi^2 n^2 \lambda^2}. \tag{13}$$

Here n is mode number and λ is defined as [15, 16]

$$\lambda^2 = \frac{1}{12\epsilon_{\text{avg}}}\frac{h^2}{l^2}, \tag{14}$$

where ϵ_{avg} is the volume-averaged static tensile strain and l is the beam length.

The derivation of Eq. 13 is based on a key insight: the flexural modes of a beam contain two vastly different length scales [9, 10]. Away from the clamping points (clamps), modes form standing waves with wavelengths on the order of $2l/n$, while near the clamping points they experience sharp bending at the length scale of λl, which is responsible for fulfilling the clamped boundary conditions $u' = 0$. As a result, the majority of the elastic energy is distributed over the mode away from the clamping points, while the small regions around them make a large (dominant for lowest-frequency modes) contribution to the intrinsic losses [14, 15]. These losses, although originating from the clamped resonator boundary, should not be confused with losses due to modal coupling to the supporting frame [31–33] or acoustic radiation [17, 34].

In the following, we refer to intrinsic loss occurring away from the clamps as the "distributed contribution" to separate these losses from the losses due to bending around the clamps.

We now generalize the multi-length scale approach for the case of non-uniform beams and derive the dissipation dilution factors as (see details in SI)

$$D_{Q,n} = \frac{1}{2\alpha_n \lambda + \beta_n \Omega_n^2 \lambda^2}, \tag{15}$$

where we introduced dimensionless frequency of n-th mode Ω_n given by

$$\Omega_n^2 = \frac{\rho l^2 \omega_n^2}{\epsilon_{\text{avg}} E}, \tag{16}$$

and beam shape-dependent clamping and distributed loss coefficients α_n and β_n are found as

$$\alpha_n = \frac{\sqrt{v_{\text{cl}}}(u'_{\text{cl},n})^2}{2\Omega_n^2\left(\int_0^1 v(s)u_n(s)^2 ds\right)}, \tag{17}$$

$$\beta_n = \frac{\int_0^1 v(s)^3 u_n(s)^2 ds}{\int_0^1 v(s)u_n(s)^2 ds}. \tag{18}$$

Here $s = x/l$ is the scaled coordinate along the beam, $u_n(s)$ is the mode shape, $v(s) = w(s)/w_{\text{avg}}$ is the beam width variation normalized to its average width and quantities with subscript "cl" are computed near the clamps (see SI).

Dissipation dilution of a non-uniform beam can be discussed entirely in terms of the reduction of the α_n and β_n coefficients by varying the beam shape $w(x)$; however, some results are more intuitively interpreted from the perspective of geometric strain engineering [19, 23, 24], a technique that exploits the relaxation of a suspended film to locally enhance the strain. Formally, the treatment in terms of the transverse beam shape, $w(x)$, or the static strain distribution along the beam, $\epsilon(x)$, is equivalent as these quantities are uniquely related as (see SI for details)

$$\epsilon(x)/\epsilon_{\text{avg}} = w_{\text{avg}}/w(x), \tag{19}$$

through the condition that the tension force must be constant along the beam.

IV. DISSIPATION DILUTION LIMIT

Before showing how dissipation dilution can be enhanced in a non-uniform beam, we derive a rigorous upper bound for D_Q. This bound is set by the yield strain, material parameters, beam thickness and the vibration frequency, but does not depend on the beam length nor the mode order. The bound is obtained by assuming the clamping contribution to intrinsic loss to be negligible ($\alpha_n = 0$) and evaluating the distributed loss coefficient β_n using the strain-width relation (Eq. 19) and the condition that the maximum strain in the beam cannot exceed

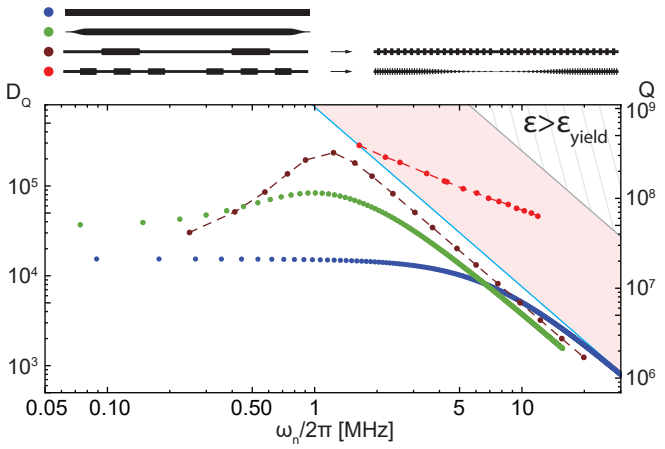

FIG. 3. Dissipation dilution in beams with different transverse profiles, assuming a fixed length $l = 3$ mm and thickness $h = 20$ nm. Points correspond to D_Q (left axis) and Q (right axis) for specific flexural modes, assuming $Q_{\rm int} = 1.4 \times 10^3$. Blue and green points correspond to modes of uniform and thin-clamped ($v_{\rm cl} = 0.14$) beams. Dark red and red points correspond to localized modes of PnC beams and tapered PnC beams, respectively. Note that each localized mode corresponds to a different beam shape. Blue line: limit for a soft-clamped beam (Eq. 22). Gray line: ultimate limit, same as D_Q for a clamp-free beam strained to the yield point (Eq. 21).

the yield strain $\epsilon_{\rm yield}$. As a result we obtain (see SI for details)

$$\beta_n \geq \left(\frac{\epsilon_{\rm avg}}{\epsilon_{\rm yield}}\right)^2, \tag{20}$$

and thus the ultimate dissipation dilution bound is given by

$$D_Q \leq \frac{12E\epsilon_{\rm yield}^2}{\rho h^2 \omega^2}. \tag{21}$$

Interestingly, while being a rigorous and general result, Eq. 21 has a simple and intuitive interpretation: dissipation dilution cannot exceed the value for an idealized clampless uniform beam strained to the yield point.

V. NON-UNIFORM BEAMS WITH ENHANCED DISSIPATION DILUTION

We consider three beam designs which produce vibrational modes with enhanced dissipation dilution compared to a uniform beam—phononic crystal (PnC) beams, beams with thin clamps and tapered PnC beams. We first analytically estimate the attainable D_Qs with these designs and then numerically calculate them by solving the Euler-Bernoulli equation [25] (see SI). Numerical calculations of dissipation dilution and quality factors are presented in Fig. 3 for beams with length $l = 3$ mm and thickness $h = 20$ nm. D_Q factors apply to beams made of any material with given pre-strain (0.46% in the figure), whereas the absolute Q factors are calculated assuming parameters typical to stoichiometric Si_3N_4 films[17, 35] ($E = 250$ GPa, $\nu = 0.23$, $\sigma_{\rm film} = 1.14$ GPa, $Q_{\rm int} = 1.4 \times 10^3$ for $h = 20$ nm), a well-established material for strained nanomechanics [16]. Note that with these extreme parameters the maximum dilution factor is large ($D_Q > 10^4$) even for a uniform beam.

The first strategy we consider is soft clamping [18, 19]—suppression of intrinsic loss around the clamps by localizing a flexural mode in a phononic crystal. A 1D phononic crystal can be formed by periodically modulating the beam width [17] (with $w_{\rm max} = 2w_{\rm min}$ for the design in Fig. 3). Localized modes of a PnC beam can closely approach the performance of idealized clamp-less beams with purely sinusoidal mode shapes, which would have dilution factors given by

$$D_Q = \frac{12E\epsilon_{\rm film}^2}{(1-\nu)^2 \rho h^2 \omega^2}. \tag{22}$$

Here Poisson's ratio accounts for relaxation of film stress in transverse direction upon suspension. Importantly, the strong suppression of mechanical mode amplitude near the clamps requires a large number of PnC unit cells and thus a high order n of the localized mode. For high-order modes, distributed losses increase as n^2 due to increased bending curvature for shorter acoustic wavelengths and at some point exceed the suppressed intrinsic loss from around clamps. These trends can be seen in Fig. 3, where the D_Q factor of the localized mode is plotted versus frequency. D_Q can be optimized by changing the localized mode order n while keeping all the parameters fixed except for the unit cell length (which changes approximately as l/n). The amplitude of a localized mode decays exponentially with the distance from the defect, such that the coefficient for intrinsic loss around clamps can be estimated as $\alpha_n = e^{-(n-1)/n_L}$, where n_L is the mode amplitude decay length in units of acoustic half-wavelengths. Optimization of D_Q in Eq. 15 with respect to n, yields

$$D_{Q,\rm max} \approx \frac{1}{\pi^2 n_{\rm max}^2 \lambda^2}, \tag{23}$$

where $n_{\rm max}$ is the optimum localized mode order, which increases only logarithmically slowly with $1/\lambda$ (see SI for the explicit expression). This result demonstrates that patterning a beam with a phononic crystal can provide an improvement in D_Q by a factor of $\sim 1/(n_{\rm max}^2\lambda)$ compared to a uniform beam of the same size. Note that the maximum attainable D_Q is far below $1/\lambda^2$—the enhancement expected from the suppression of the clamping contribution to intrinsic loss for a fundamental mode—as $n_{\rm max}$ is in practice much greater than 1. It also follows from Eq. 23 that in order for soft clamping to provide an increased quality factor, λ needs to be much smaller than 1, i.e. dissipation dilution factors needs to be high even for non-localized modes.

The second strategy we consider is reduction of the beam width near the clamps, $v_{\rm cl} = w(0)/w_{\rm avg}$, in order to

create local strain enhancement in the clamping regions (see Fig. 2A top). Eq. 17 shows that α_n is proportional to $\sqrt{v_{\rm cl}}$ and thus can be reduced by thinning down the clamps ($u'_{{\rm cl},n}$ and Ω_n are almost unaffected by $v_{\rm cl}$ as long as the clamping region length is small). This can be interpreted as an effective decrease of λ over the clamping region to

$$\lambda_{\rm cl} = \sqrt{h^2/12\epsilon_{\rm cl} l^2}, \tag{24}$$

where $\epsilon_{\rm cl} = \epsilon_{\rm avg}/v_{\rm cl}$ is the local strain. The dissipation dilution of beams with thin clamps is thus given by

$$D_{Q,n} \approx \frac{1}{2\lambda_{\rm cl} + (n\pi)^2\lambda^2}. \tag{25}$$

In contrast to the PnC approach, thin-clamping beams are predicted to have improved quality factors for low-order beam modes, including the fundamental mode (see Fig. 3, green points).

One caveat needs to be mentioned when considering the effect of local strain on dissipation dilution: geometric concentration of strain in one region unavoidably results in the reduction of strain elsewhere. To improve dilution factors beyond those of a uniform beam, the region(s) of enhanced strain must overlap with the region(s) which dominate dissipation in the vibrational mode, in this case the clamps. A common beam geometry which does not satisfy this requirement, a beam with filleted (thick) clamping points, is shown in the bottom of Fig. 2A. This result is at odds with recently reported enhanced Qs in trampoline membranes with filleted tethers [36].

In both uniform PnC and thin-clamped beams, the clamping contribution to intrinsic loss is reduced, but the distributed contribution is not. The latter can be addressed by co-localization of both the flexural mode and the strain away from the clamps as shown in Fig. 2B. Following the strategy described in [19], here the width of the PnC is changed cell-wise according to

$$w_{{\rm cell},i} \propto 1 - (1-a)\exp(-i^2/i_0^2), \tag{26}$$

where $i = 0, 1 ...$ is the cell index starting from the beam center, a and i_0 respectively define the transverse and longitudinal sizes of the waist region. Importantly, the PnC cell lengths must also be scaled proportional to $1/\sqrt{w_{\rm cell}}$ in order to compensate for the bandgap frequency shift due to the non-uniform strain distribution.

An estimate of D_Q for the tapered PnC is obtained by assuming that the mode is localized in the waist region of width $v_{\rm waist}$ and that the clamping contribution to intrinsic loss is negligible:

$$D_{Q,n} \approx \frac{1}{\Omega_{\rm waist}^2 \lambda_{\rm waist}^2}, \tag{27}$$

where

$$\Omega_{\rm waist} = \sqrt{\rho l^2 \omega^2/(\epsilon_{\rm waist} E)}, \tag{28}$$

$$\lambda_{\rm waist} = \sqrt{h^2/(12\epsilon_{\rm waist} l^2)}, \tag{29}$$

and $\epsilon_{\rm waist} = \epsilon_{\rm avg}/v_{\rm waist}$. It follows that by increasing the waist strain to the yield value, the ultimate limit of dissipation dilution (Eq. 21) is attainable with tapered PnC beam designs, in contrast to the previous two methods.

A practical limitation for dissipation dilution enhancement by strain concentration in this case originates from the tradeoff between $\epsilon_{\rm waist}$ and the waist length. Substantially increased strain is only achievable over a small fraction of the beam length, therefore only short-wavelength and high-frequency modes can benefit from such global geometric strain engineering. In Fig. 3 we plot D_Q versus frequency for localized modes of tapered beams, where the taper waist has been adjusted to match the wavelength of the localized mode. It can be seen that as the mode frequency increases, its dilution is progressively enhanced relative to conventional soft-clamped modes (red points).

VI. THERMAL NOISE LIMITS FOR FREQUENCY AND FORCE MEASUREMENTS

The quality factor of a mechanical resonator determines the uncertainty in frequency and force measurements due to the resonator's Brownian motion[28, 37, 38]. Therefore dissipation dilution directly improves these fundamental sensitivity limits. In the case of force measurements, a nanobeam is a particularly advantageous kind of resonator due to its low mass. For the highest-Q nanobeams that were experimentally demonstrated at room temperature[19], with a Q of $8 \cdot 10^8$ at 1.3 MHz (in agreement with the theory presented here within 30%) and effective mass of 11 pg, the thermal noise limit is

$$\delta F_{\rm th} = \sqrt{4k_B T m \Gamma_n} = 1.4\,{\rm aN}/\sqrt{\rm Hz} \tag{30}$$

at $T = 300\,{\rm K}$. Here $\Gamma_n = \omega_n/Q$ is the resonance linewidth. For the highest-Q soft-clamped mode in Fig. 3 ($\omega_n/(2\pi) = 1.3$ MHz, $Q = 3.3 \cdot 10^8$), assuming a beam center width of 400 nm, the force sensitivity is $\delta F_{\rm th} = 2.1\,{\rm aN}/\sqrt{\rm Hz}$. These low numbers are not only a consequence of high Q, but also of the mode localization by the phononic crystal. Modes of a beam with thin clamping points (green points in Fig. 3) have three times higher thermal noise, $\delta F_{\rm th} = 6.6\,{\rm aN}/\sqrt{\rm Hz}$ for the mode with $Q = 1.1 \cdot 10^8$ at $\omega_n/(2\pi) = 1$ MHz assuming the same beam width. The mode of a uniform beam of the same dimensions at the same frequency has quality factor $Q = 3.3 \cdot 10^7$ and force sensitivity $\delta F_{\rm th} = 12\,{\rm aN}/\sqrt{\rm Hz}$.

The thermal noise limit for an oscillator frequency measurement is more ambiguous to define in absolute terms, since here the resolution in general depends on the amplitude of the drive[37, 39] which is typically limited by the onset of nonlinearity. For flexural modes of thin beams and membranes the dominant source of nonlinearity at large amplitudes is not material but geometric nonlinearity[40], the same which creates dissipation dilution. Therefore we can estimate the contribution of

Brownian motion to oscillator frequency noise by assuming that the amplitude of driven motion is such that the nonlinear part of the energy is of the same order of magnitude as the linear part. This is equivalent to the condition that the average kinetic energy approaches the static elastic energy, $\langle W_{\rm kin}\rangle = W_{\rm el.stat.}$,

$$m_{\rm eff}\omega_n^2\langle X_{\rm osc}^2\rangle \simeq V_{\rm eff}\epsilon_{\rm avg}^2/E. \tag{31}$$

Here $m_{\rm eff}$ and $V_{\rm eff} = m_{\rm eff}/\rho$ are the effective resonator mass and volume, respectively, X is the oscillator position and $\langle X_{\rm osc}^2\rangle$ is the magnitude of driven motion. The frequency noise spectrum due to Brownian motion is given by[39]

$$S_{\omega\omega}[\omega] = 2\frac{\langle X_{\rm th}^2\rangle}{\langle X_{\rm osc}^2\rangle}\Gamma_n\frac{\omega^2}{\omega^2+(\Gamma_n/2)^2}, \tag{32}$$

where $\langle X_{\rm th}^2\rangle$ is the magnitude of the thermal fluctuations. Using Eq. 31, we estimate the minimum frequency noise (at $\omega \gg \Gamma$) as

$$S_{\omega\omega} \simeq \frac{k_B T}{W_{\rm el.stat.}}\Gamma_n. \tag{33}$$

From Eq. 33, we see that static strain reduces Brownian frequency noise in two ways—by reducing the resonator linewidth and by increasing the driving amplitude threshold at which nonlinearity comes into play. Plugging in numbers from Fig. 3 we find that the highest-Q soft-clamped mode has minimum frequency noise $\sqrt{S_{\omega\omega}}/(2\pi) \simeq 4\cdot 10^{-7}$ Hz/$\sqrt{\rm Hz}$. If converted to phase noise, this is equivalent to -230 dBc/Hz at 20 kHz offset, which is an extremely low level.

Practically, other factors than Brownian motion almost always limit the frequency stability of mechanical resonators, in particular of silicon nitride nanobeams[40]. On the other hand, in nanobeams extraneous frequency noises of different modes are highly correlated, which made it possible to demonstrate Brownian-noise limited frequency measurements with moderate-Q resonators using feedback[39]. Therefore the attainability of the Brownian noise limit in frequency measurements using ultra-high Q beams remains an open question.

VII. CONCLUSIONS AND OUTLOOK

We have presented a theoretical framework to analyze the quality factors of strained mechanical resonators of arbitrary three dimensional geometry and shown that a lossless contribution to the elastic energy, giving rise to Q-enhancement by dissipation dilution, emerges in the presence of static strain and geometric nonlinearity. High aspect ratio beams and membranes can produce particularly large dissipation dilution, though it is not impossible that other geometries can do it as well.

For the specific case of variable cross-section beams subjected to axial tension we presented an analytical model. We showed that by corrugating the beam it is possible to create modes with quality factors enhanced by more than an order of magnitude compared to a uniform beam. We interpret the Q enhancement in terms of the suppression of clamping contribution to intrinsic loss and local strain engineering, deriving the limits of each approach, and estimating practically achievable absolute Q factors for devices made of high-stress Si_3N_4. In order to perform numerical calculations for beams we developed a freely available `Mathematica` package[25].

We note that while Si_3N_4 is currently the most popular material for strained nanomechanics — particularly for applications in optomechanics [41–44] — the principles described here apply to resonators made of any material under strain, whether produced by external force [45], lattice mismatch (e.g. during epitaxial growth) [46, 47] or mismatch of thermal expansion coefficients [48].

ACKNOWLEDGEMENTS

We thank Alexander Tagantsev for useful discussions. This work was supported by the EU Horizon 2020 Research and Innovation Program under grant agreement no. 732894 (FET-Proactive HOT), the Swiss National Science Foundation (grant no. 182103) and the Defense Advanced Research Projects Agency (DARPA), Defense Sciences Office (DSO) under contract no. HR0011181003. M.J.B. acknowledges support from the EU Horizon 2020 research and innovation programme under the Marie Sklodowska-Curie grant agreement No. 722923 (OMT). Code to reproduce data in Fig. 2 and Fig. 3 is available on Zenodo[25].

[1] L. Ju, D. G. Blair, and C. Zhao, Reports on Progress in Physics **63**, 1317 (2000).
[2] M. Aspelmeyer, T. J. Kippenberg, and F. Marquardt, Reviews of Modern Physics **86**, 1391 (2014).
[3] R. W. Andrews, R. W. Peterson, T. P. Purdy, K. Cicak, R. W. Simmonds, C. A. Regal, and K. W. Lehnert, Nature Physics **10**, 321 (2014).
[4] T. Bagci, A. Simonsen, S. Schmid, L. G. Villanueva, E. Zeuthen, J. Appel, J. M. Taylor, A. Srensen, K. Us-

ami, A. Schliesser, and E. S. Polzik, Nature **507**, 81 (2014).
[5] A. Vinante, R. Mezzena, P. Falferi, M. Carlesso, and A. Bassi, Physical Review Letters **119**, 110401 (2017).
[6] D. Rugar, R. Budakian, H. J. Mamin, and B. W. Chui, Nature **430**, 329 (2004).
[7] Y. T. Yang, C. Callegari, X. L. Feng, K. L. Ekinci, and M. L. Roukes, Nano Letters **6**, 583 (2006).
[8] H. B. Callen and T. A. Welton, Physical Review **83**, 34 (1951).
[9] G. Gonzlez, Classical and Quantum Gravity **17**, 4409 (2000).
[10] G. I. González and P. R. Saulson, The Journal of the Acoustical Society of America **96**, 207 (1994).
[11] S. S. Verbridge, J. M. Parpia, R. B. Reichenbach, L. M. Bellan, and H. G. Craighead, Journal of Applied Physics **99**, 124304 (2006).
[12] B. M. Zwickl, W. E. Shanks, A. M. Jayich, C. Yang, A. C. Bleszynski Jayich, J. D. Thompson, and J. G. E. Harris, Applied Physics Letters **92**, 103125 (2008).
[13] Q. P. Unterreithmeier, E. M. Weig, and J. P. Kotthaus, Nature **458**, 1001 (2009).
[14] Q. P. Unterreithmeier, T. Faust, and J. P. Kotthaus, Physical Review Letters **105**, 027205 (2010).
[15] P.-L. Yu, T. P. Purdy, and C. A. Regal, Physical Review Letters **108**, 083603 (2012).
[16] L. Villanueva and S. Schmid, Physical Review Letters **113**, 227201 (2014).
[17] A. H. Ghadimi, D. J. Wilson, and T. J. Kippenberg, Nano Letters (2017), 10.1021/acs.nanolett.7b00573.
[18] Y. Tsaturyan, A. Barg, E. S. Polzik, and A. Schliesser, Nature Nanotechnology **12**, 776 (2017).
[19] A. H. Ghadimi, S. A. Fedorov, N. J. Engelsen, M. J. Bereyhi, R. Schilling, D. J. Wilson, and T. J. Kippenberg, Science **360**, 764 (2018).
[20] T. Capelle, Y. Tsaturyan, A. Barg, and A. Schliesser, Applied Physics Letters **110**, 181106 (2017).
[21] R. A. Minamisawa, M. J. Sess, R. Spolenak, J. Faist, C. David, J. Gobrecht, K. K. Bourdelle, and H. Sigg, Nature Communications **3**, 1096 (2012).
[22] V. B. Braginsky, V. P. Mitrofanov, and V. I. Panov, *Systems with Small Dissipation* (University of Chicago Press, 1985).
[23] T. Zabel, R. Geiger, E. Marin, E. Mller, A. Diaz, C. Bonzon, M. J. Sess, R. Spolenak, J. Faist, and H. Sigg, Journal of Materials Research **32**, 726 (2017).
[24] R. Zhang, C. Ti, M. I. Davano, Y. Ren, V. Aksyuk, Y. Liu, and K. Srinivasan, Applied Physics Letters **107**, 131110 (2015).
[25] Mathematica package is available at zenodo.com, DOI:10.5281/zenodo.1296925.
[26] T. Corbitt, C. Wipf, T. Bodiya, D. Ottaway, D. Sigg, N. Smith, S. Whitcomb, and N. Mavalvala, Physical Review Letters **99**, 160801 (2007).
[27] K.-K. Ni, R. Norte, D. J. Wilson, J. D. Hood, D. E. Chang, O. Painter, and H. J. Kimble, Physical Review Letters **108**, 214302 (2012).
[28] P. R. Saulson, Physical Review D **42**, 2437 (1990).
[29] L. D. Landau and E. M. Lifshitz, *Theory of elasticity* (London Pergamon Press, 1970).
[30] See Supplemental Material at [URL will be inserted by publisher] for more general and detailed derivations, in-depth descriptions of nanobeam spectra and comparison between the numeric methods used.
[31] I. Wilson-Rae, R. A. Barton, S. S. Verbridge, D. R. Southworth, B. Ilic, H. G. Craighead, and J. M. Parpia, Physical Review Letters **106**, 047205 (2011).
[32] G. D. Cole, I. Wilson-Rae, K. Werbach, M. R. Vanner, and M. Aspelmeyer, Nature Communications **2**, 231 (2011).
[33] Y. Tsaturyan, A. Barg, A. Simonsen, L. G. Villanueva, S. Schmid, A. Schliesser, and E. S. Polzik, Optics Express **22**, 6810 (2014).
[34] J. Chan, A. H. Safavi-Naeini, J. T. Hill, S. Meenehan, and O. Painter, Applied Physics Letters **101**, 081115 (2012).
[35] S. A. Fedorov, V. Sudhir, R. Schilling, H. Schtz, D. J. Wilson, and T. J. Kippenberg, Physics Letters A Special Issue in memory of Professor V.B. Braginsky, **382**, 2251 (2018).
[36] R. Norte, J. Moura, and S. Grblacher, Physical Review Letters **116**, 147202 (2016).
[37] U. Drig, O. Zger, and A. Stalder, Journal of Applied Physics **72**, 1778 (1992).
[38] D. Ramos, J. Tamayo, J. Mertens, M. Calleja, L. G. Villanueva, and A. Zaballos, Nanotechnology **19**, 035503 (2007).
[39] E. Gavartin, P. Verlot, and T. J. Kippenberg, Nature Communications **4**, 2860 (2013).
[40] K. Y. Fong, W. H. P. Pernice, and H. X. Tang, Physical Review B **85**, 161410 (2012).
[41] J. D. Thompson, B. M. Zwickl, A. M. Jayich, F. Marquardt, S. M. Girvin, and J. G. E. Harris, Nature **452**, 72 (2008).
[42] D. J. Wilson, C. A. Regal, S. B. Papp, and H. J. Kimble, Physical Review Letters **103**, 207204 (2009).
[43] T. P. Purdy, R. W. Peterson, and C. A. Regal, Science **339**, 801 (2013).
[44] D. J. Wilson, V. Sudhir, N. Piro, R. Schilling, A. Ghadimi, and T. J. Kippenberg, Nature **524**, 325 (2015).
[45] S. S. Verbridge, D. F. Shapiro, H. G. Craighead, and J. M. Parpia, Nano Letters **7**, 1728 (2007).
[46] G. D. Cole, P.-L. Yu, C. Gärtner, K. Siquans, R. Moghadas Nia, J. Schmöle, J. Hoelscher-Obermaier, T. P. Purdy, W. Wieczorek, C. A. Regal, *et al.*, App. Phys. Lett. **104**, 201908 (2014).
[47] A. Moridi, H. Ruan, L. C. Zhang, and M. Liu, International Journal of Solids and Structures **50**, 3562 (2013).
[48] C. A. Regal, J. D. Teufel, and K. W. Lehnert, Nature Physics **4**, 555 (2008).